ORIGINAL PAPER

The network gel polymer electrolyte based on poly(acrylate-*co*-imide) and its transport properties in lithium ion batteries

**Fu-Ming Wang · Jyh-Tsung Lee · Ju-Hsiang Cheng ·
Chin-Shu Cheng · Chang-Rung Yang**

Abstract Poly (acrylate-*co*-imide)-based gel polymer electrolytes are synthesized by in situ free radical polymerization. Infrared spectroscopy confirms the complete polymerization of gel polymer electrolytes. The ionic conductivity of gel polymer electrolytes are measured as a function of different repeating EO units of polyacrylates. An optimal ionic conductivity of the poly (PEGMEMA$_{1100}$-BMI) gel polymer electrolyte is determined to be 4.8×10^{-3} S/cm at 25 °C. The lithium transference number is found to be 0.29. The cyclic voltammogram shows that the wide electrochemical stability window of the gel polymer electrolyte varies from −0.5 to 4.20 V (vs. Li/Li$^+$). Furthermore, we found the transport properties of novel gel polymer electrolytes are dependent on the EO design and are also related to the rate capability and the cycling ability of lithium polymer batteries. The relationship between polymer electrolyte design, lithium transport properties and battery performance are investigated in this research.

F.-M. Wang (✉) · C.-S. Cheng · C.-R. Yang
Material and Chemical Research Laboratories,
Industrial Technology Research Institute,
Rm.405, Bldg. 77, 195 Sec. 4, Chung Hsing Rd., Chutung,
Hsinchu 310, Taiwan
e-mail: mccabe@itri.org.tw

J.-T. Lee
Department of Chemistry and Center for Nano Science
and Technology, National Sun Yat-Sen University,
Kaohsiung, Taiwan

F.-M. Wang · J.-H. Cheng
Department of Chemical Engineering,
National Tsing Hua University,
Hsinchu, Taiwan

Introduction

Lithium polymer secondary batteries using gel polymer electrolytes have attracted a great deal of attention due to their high energy density and reliability [1–11]. Gel polymer electrolytes can be classified into two categories according to their physical and chemical cross-links [12]. To satisfy these rigorous requirements, researchers have explored the design of polymer electrolytes [13] which consist of two chemically dissimilar polymers covalently bonded end-to-end. Typically, the chemical cross-linked gel electrolytes consist of a liquid solution and a network polymer. The precursors of the polymer are monomers and a cross-linker. The matrices of the polymer electrolytes are poly (ethylene oxide) (PEO) [14], poly (methyl methacrylate) (PMMA) [15], poly (acrylonitrile) (PAN) [16], and poly (vinylidene fluride) (PVdF) [17]. The copolymers such as PVdF-HFP have already been investigated [17]. As for the cross-linker, it should have more than two functional groups to react with other molecules to form a three-dimensional network polymer, which could absorb the liquid electrolytes. Usually, the cross-linkers used are poly(ethylene glycol) dimethacrylate (PEGDMA) [18]. Nevertheless, the ionic conductivity of gel polymer electrolytes with those kinds of cross-linkers is always below 3×10^{-3} S/cm at 25 °C [19]. This is because the cross-linkers will suppress the vibration of the polymer chains. The lower ionic conductivity will increase the concentration polarization of gel polymer electrolytes resulting in decrease to the power density of lithium batteries. The Samsung SDI developed some new gel electrolytes by using poly (ethylene glycol) diacrylate (PEGDA) and PEGDMA as

the cross-linking agents, in which the chemical and physical properties were similar to ours, but the problem of ionic conductivity and crystallization reduced the cell performance, especially the 2C discharge below 80% [20].

In this paper, we have introduced bismaleimide (BMI) as the cross-linking agent in our gel polymer electrolyte, and it provides rigid structure and hydrophobic chemistry. However, BMI has a three dimensional obstacles and cannot polymerize to a flexible film. Accordingly, we used methacylates as a monomer and bismaleimide as a cross-linker to fabricate a three-dimensional polymer, poly (acrylate-co-imide), via in situ polymerization. It has been reported that BMI epoxy resin has good thermal and mechanical properties because of its superior chain rigidity, excellent thermal and thermo oxidative stability, and negligible tendency to absorb water [21]. The resulting gel polymer electrolytes of poly (acrylate-co-imide) have a higher ionic conductivity than typical gel polymer electrolytes [22]. We also investigated the effects of the polymer contents of gel polymer electrolytes on the ionic conductivity. The electrochemical properties of the gel polymer electrolytes were also studied. Furthermore, the gel polymer electrolytes were also applied to advanced batteries in order to study their electrochemical properties.

Experimental

Materials

Methyl methacrylate and poly (ethylene glycol) methyl ether methacrylate (PEGMEMA$_{475}$, Mn=475 and PEG-MEMA$_{1100}$, Mn=1,100) were purchased from Aldrich. All of the acrylates were dried prior to use by using silica gel and also distilled before use. The initiator, 2,2′-azobisisobutyronitrile (AIBN), was supplied by Showa and dried in the vacuum for 72 h. Bismaleimide was purchased from Acros Organics. Ethylene carbonate (EC), propylene carbonate (PC), diethyl carbonate (DEC), and lithium hexafluorophosphate (LiPF$_6$) were electrochemical grades from Ferro.

Preparation of gel polymer electrolytes

Acrylates (MMA, PEGMEMA$_{475}$, or PEGMEMA$_{1100}$) and BMI (1:1 by weight) were dissolved in a mixture solvent of EC–PC–DEC (3:2:5 by volume). LiPF$_6$ as the salt was added to the above solution to achieve a concentration of 1.0 M and mixed homogeneously. The initiator was then added to the solution mixture. The composition weight ratio of mixed monomers (acrylates and BMI)/initiator was 200/1. The solution show a light yellow color and prepared as above was poured into a Teflon mold at 90 °C in the oven for 1 h to form a gel polymer electrolyte. All the chemicals stored and polymerizations were in the glove box with inert atmosphere.

Instrumentation

The gel polymer electrolyte was characterized using Infrared (IR) spectroscopy (Bomem, DA-8.3 FTS). Ionic conductivities were measured by AC impedance spectroscopy using a Solatron impedance analyzer (SI-1260) in combination with electrochemical interface (SI-1286) potentiostat/galvanostat in the frequency range from 0.1–100 kHz, AC amplitude of 10 mV, and a temperature range of 25–90 °C. Control of the equipment was done using a Z-Plot electrochemical software purchased from Solatron, Inc. Temperature-dependent conductivities were obtained by placing the electrochemical cell in an oven. At high temperatures/conductivities, impedance spectra were slanted lines; at low temperatures/conductivities, impedance spectra consisted of depressed semicircles at higher frequencies and slanted lines at lower frequencies. The resistance was obtained from the intercept of the slanted line extrapolated to the real axis of the impedance spectra plots (imaginary (Z') vs. real (Z')). The specific ionic conductivity, σ, was obtained from σ=l/AR, where l is the distance between the two stainless steel electrodes (0.5 cm), A is the area (1 cm^2), and R is the resistance (Ω). The compatibility of polymer electrolytes with the stainless electrode was determined via AC impedance analysis under open-circuit conditions at different temperatures. The electrochemical stability of gel polymer electrolytes was measured by cyclic voltammetry (CV) using a Solatron 1287 between −0.5 to 2 V and 2.75 to 4.2 V at a scan rate of 0.5 mV s^{-1} using a three-electrode cell, consisting of one stainless steel working electrode in an area of 1.0 cm^2 and lithium counter and reference electrodes. The gel polymer electrolyte filled the space between working and counter electrodes.

The transference number of the lithium ion, t_{Li}^+, was determined by the method of Evans [23–24]. According to this method, the electrolyte was put into two lithium electrodes. DC voltage (ΔV=10 mV) was applied to these two electrodes until the current became a steady-state value. The AC impedance measured the resistance of the polymer electrolyte and the interface before/after the voltage was applied (unclear). The t_{Li}^+ was calculated with the following formula:

$$t_{Li}^+ = I_{ss}(\Delta V - I_o R_o)/I_o(\Delta V - I_{ss}R_{ss})$$

where ΔV is the potential applied across the cell. I_o and I_{ss} are, respectively, the initial and the steady-state currents during the polarization. R_o and R_{ss} are the interfacial resistance at the initial and steady states, respectively.

Battery performance testing

Advanced lithium-ion batteries (ALB, aluminum-plastic laminated film exterior with dimensions of 3.8 ×35 ×

62 mm) were used in this work. LiCoO$_2$ (LiCo) was used for the cathode and MCMB (modification of mesocarbon microbeads) (China Steel Chemical) electrode was used as the anode. A separator (Celgard 2320) was placed between the cathode and the anode. The gel polymer electrolyte was filled to a predetermined weight. Batteries were charged at a constant current of 0.2 °C to 4.2 V and discharged at 0.2 °C, 1 °C, and 2 °C to 2.75 V. To measure the cycle ability, batteries were cycled at 0.2 °C between 2.75 V and 4.2 V.

Results and discussion

Characterization of polymer electrolytes

The poly (acrylate-*co*-imide)-based gel polymer electrolytes were synthesized by in situ polymerization, as shown in Fig. 1. In this study, we used acrylate as a monomer and

BMI as a cross-linker to establish a three-dimensional network copolymer. Therefore, the liquid electrolyte can be absorbed in the three-dimensional network copolymer to form a gel polymer electrolyte. The polymerization of the gel polymer electrolytes was characterized by FT-IR. Figure 2 shows the gel polymer electrolyte before and after polymerization. It obviously shows that the C=C stretching of acrylate and that of C=C of imide absorb at 1,638 cm^{-1}, and the C=O stretching of BMI occurs at 1,651 cm^{-1}. After polymerization at 90 °C for 1 h, the C=C stretching of acrylate almost disappeared and the wave number of the C=O stretching changed to 1,721 cm^{-1} for the acrylate and from 1,651 cm^{-1} for BMI to 1,731 cm^{-1} for the poly (acrylate-*co*-imide). These changes are due to the conjugated C=O transforming to an isolated C=O polymerization. The IR result implies that the C=C bonds can be broken and polymerization proceeds only when the temperature is well above 90 °C.
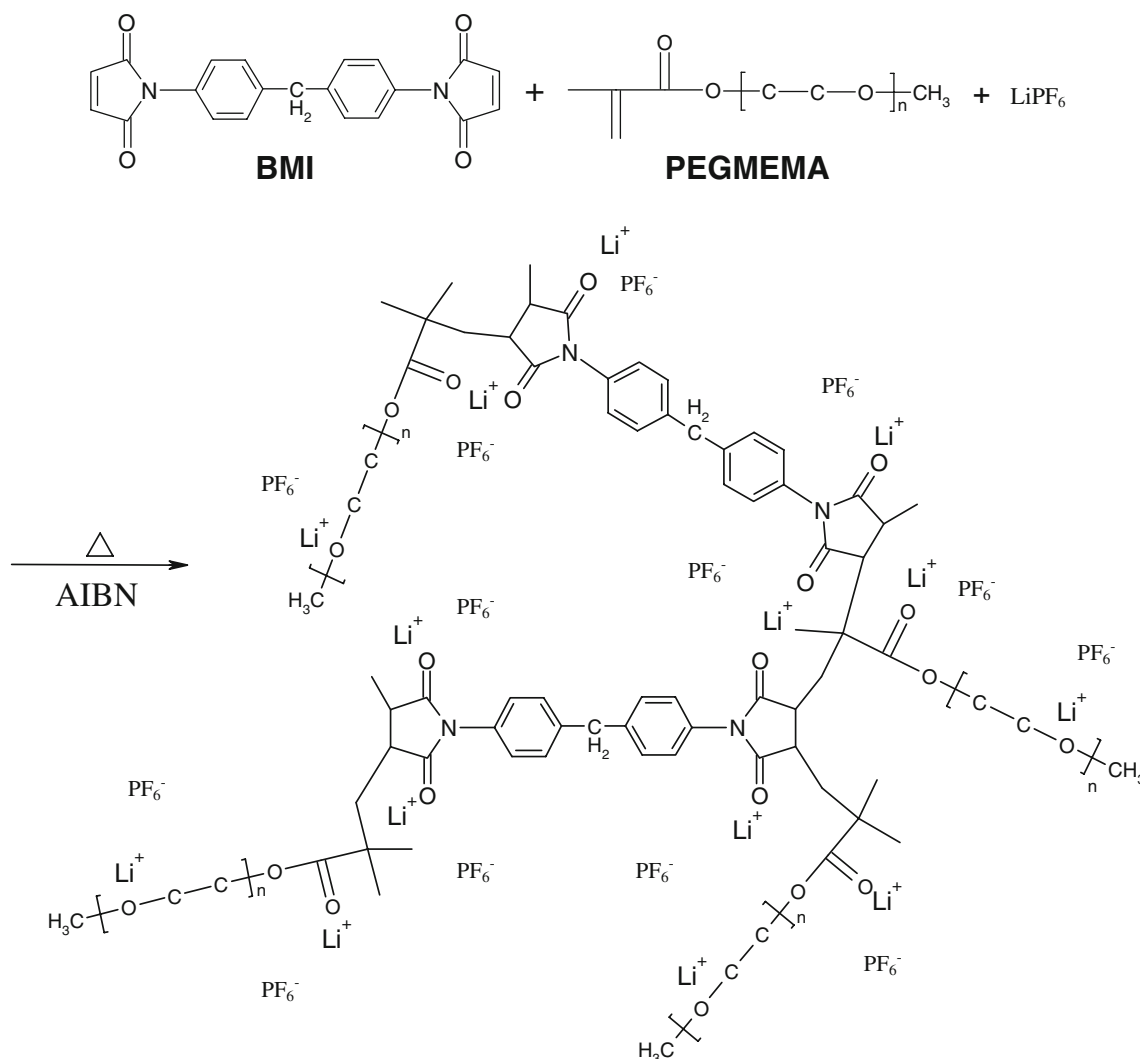
Fig. 1 Synthesis of intercross linked gel polymer electrolytes
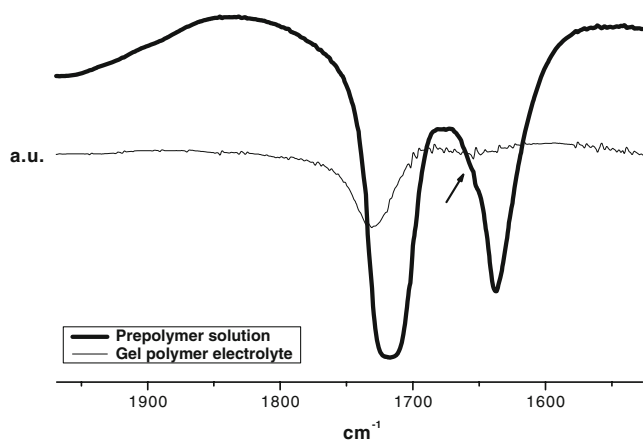
Fig. 2 FT-IR spectra of 10 wt.% poly (PEGMEMA$_{450}$-BMI) gel electrolytes showing before and after thermal polymerization

Ionic conductivity analysis

PEGMEMA (poly (ethylene glycol) methyl ether methacrylate) has been synthesized to BMI first time, and provide different EO side chain as flexible backbone of the electrolyte structure to contact perfectly with the active material. According to our present research, which is compared the different of cross-linked agent by in-situ polymerization. Although PEGDMA has also an EO chain in the structure, the ionic conductivity is less than our copolymer which the reason consists in the EO repeat unit is also the main chain of polymer. Furthermore, the EO units at the main chain of the polymer electrolyte will incur serious crystallization. Such a process will reduce the ionic transfer of lithium ion compared to our poly (imide-acrylate) gel electrolyte. The ionic conductivity of poly (PMMA-PEGDMA) is 3.9 mS/cm at 25 °C, which is less than that of poly (PMMA-BMI).

Figure 3 shows the ionic conductivity of gel polymer electrolytes with 10 wt % of poly (MMA-BMI), poly (PEGMEMA$_{475}$-BMI) and poly (PEGMEMA$_{1100}$-BMI) at various temperatures. For the low temperature region, the poly (MMA-BMI) gel electrolyte has a higher ionic conductivity than poly (PEGMEMA$_{450}$-BMI) and poly (PEGMEMA$_{1100}$-BMI) electrolytes. By contrast, the poly (PEGMEMA$_{1100}$-BMI) has the highest ionic conductivity in the high temperature region. This appearance is shown that the EO side chains vibrate differently at low temperatures. However, the polymerized MMA has a longer distance between crossed points than poly (PEGMEMA$_{450}$) and poly (PEGMEMA$_{1100}$) though their weights are the same. Therefore, the backbone of polymer chains of poly (MMA-BMI) vibrates more readily at low temperatures resulting in a higher ionic conductivity at room temperature. In addition, this figure also indicates that a longer EO side chain produced better ionic motion with lithium ion

transfer at high temperature due to the longer EO side chain for the flexible structure of mechanical properties.

Figure 4 shows the ionic conductivity with different percentage of poly (MMA-BMI), poly (PEGMEMA$_{450}$-BMI) and poly (PEGMEMA$_{1100}$-BMI) electrolytes at 25 °C. The ionic conductivities of the electrolytes shows low percentage polymer of poly (MMA-BMI) were higher than the others. These phenomena display the higher polymer content obstructing the transport of lithium ions in electrolytes. However, the poly (PEGMEMA$_{1100}$-BMI) is provided the sensitive motion of the EO side chain at high temperature due to their soft backbone of structure. Therefore, the overall results combined with Figs. 3 and 4 are showing the EO design is a very important topic for battery application. Figure 5 shows the phase angle of the 10 and 20 wt.% addition of poly (PEGMEMA$_{1100}$-BMI) decreased compare to the poly (PEGMEMA$_{475}$-BMI). This result indicated that although the polymer electrolyte with 10 or 20 wt.% addition of poly (PEGMEMA$_{1100}$-BMI), the ionic conductivity effect are still dominated by liquid electrolyte with 10 wt.% addition (poly (PEGMEMA$_{475}$-BMI)>poly (PEGMEMA$_{1100}$-BMI)). However, the EO in polymer effect is starting from 20 wt.% addition, which the ionic conductivity of poly (PEGMEMA$_{1100}$-BMI) is better than poly (PEGMEMA$_{475}$-BMI).

Cyclic voltammetry analysis

Typical cyclic voltammetry curves of the poly (acrylate-co-imide)-based gel electrolytes with different acrylates are determined in the range from −0.5 to 2 V (vs. Li/Li$^+$) and 2.75 to 4.2 V are shown in Figs. 6 and 7, respectively. The background current densities do not show significant amount of decomposition current in the first profiles.
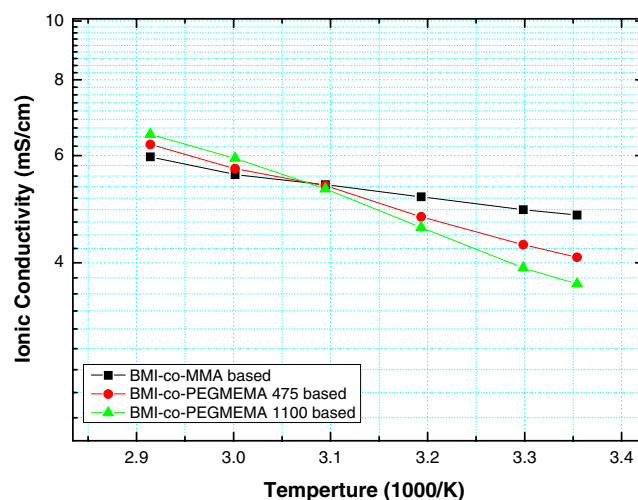
Fig. 3 The 10 wt.% additional gel electrolytes of EO side chain dependence of ionic conductivity measurement at different temperatures
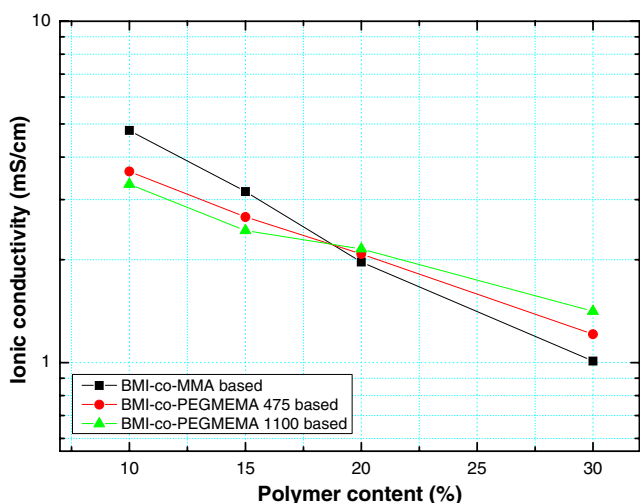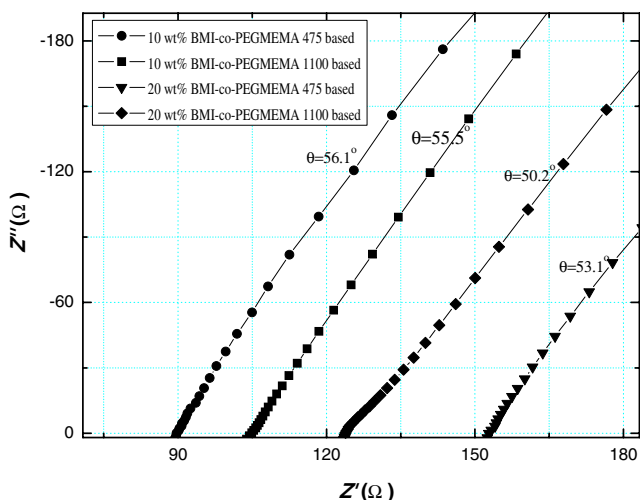
Fig. 4 The various additional polymer content gel electrolytes of EO side chain dependence of ionic conductivity measurement at room temperature

Fig. 6 Cyclic voltammograms of stainless steel/poly (PEGMEMA$_{475}$-BMI) gel electrolytes/Li; lithium plating/stripping on the stainless steel electrode for the polymer block electrolytes are shown. Working and counter electrode, stainless steel; reference electrode, lithium; scan rate=0.5 mV/s
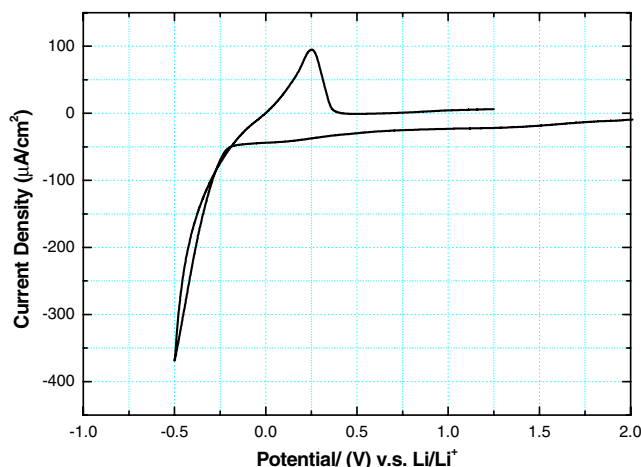
Faradaic current in the latter profile showed good cycle ability by calculating the integral area during the lithium plating and stripping scans. These results indicate that the gel electrolytes have a potential window wide enough for using in a lithium ion battery.

Transference number analysis

Both ionic conductivity and lithium transference number are important to the polymer electrolyte designed. There are several methods (for example, AC impedance spectroscopy, potentiometric measurements, and nuclear magnetic resonance) available to determine the lithium transference number in polymer electrolytes. As shown in Table 1, a constant potential, 10 mV (ΔV), was applied across the Li/

gel polymer electrolyte/Li cell until the current (I_{ss}) reached a steady-state value and the interfacial resistance was measured before (R_o) and after (R_{ss}) the applied potential. The t_{Li}^+ of all the samples displayed somewhat high values when compared to other PEO-based polymer electrolytes. Vincent et al. [25] and Abraham et al. [26] obtained t_{Li}^+ of about 0.6 for a PEO-LiClO$_4$-TiO$_2$ polymer electrolyte using the same method. The gel polymer electrolytes were 1 M LiPF$_6$ in our liquid electrolyte with 10 and 20 wt.% polymers. As far as the t_{Li}^+ of our electrolytes with 10 wt % poly (PEGMEMA$_{1100}$-BMI) is measured, the t_{Li}^+ of the gel polymer electrolyte with the longest EO repeat units (0.29) is lower than 10 wt.% poly (MMA-BMI) (0.36) and 20 wt.% poly (MMA-BMI) (0.33), respectively. We caused the EO repeat units to drop T_g which is determined by DSC
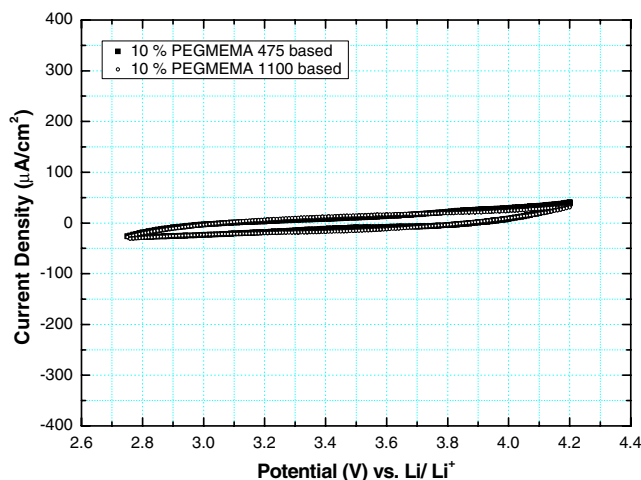

Fig. 5 Nyquist plots of poly (acrylate-co-imide)-based gel polymer electrolytes measured at room temperature
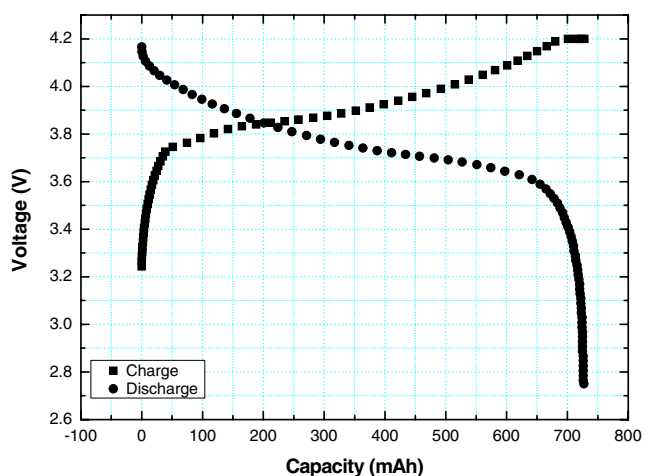

Fig. 7 Cyclic voltammograms of stainless steel/ poly (PEGMEMA-BMI) gel electrolytes/Li. Working and counter electrode, stainless steel; reference electrode, lithium; scan rate=0.5 mV/s
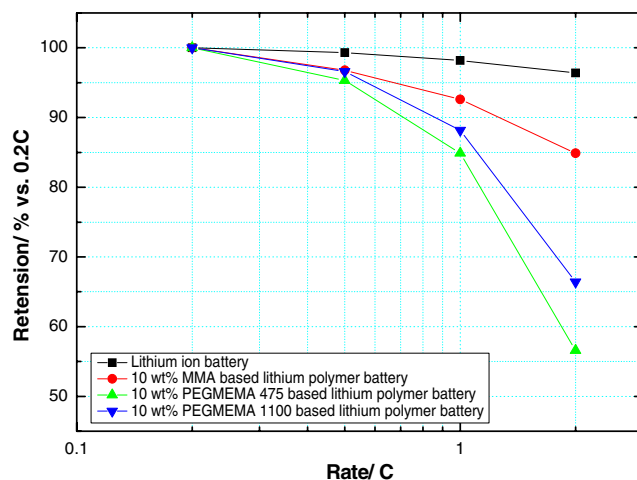
Table 1 Parameter obtained from the application of a constant potential and impendence to calculate the lithium transference number of gel polymer electrolytes. There measurements were carried out at 25 °C

Polymer type	t^+
10 wt.% poly (MMA-BMI)	0.36
20 wt.% poly (MMA-BMI)	0.33
10 wt.% poly (PEGMEMA$_{1100}$-BMI)	0.29
20 wt.% poly (PEGMEMA$_{1100}$-BMI)	0.22

test and assist the carrier ions through to the polymer structure, however, the longest EO repeat units also restrict the carrier ions transportation by the three dimensional baffle. There are two results assembled from our data. First, we used MMA and BMI as a copolymer, and BMI is not only a cross-linking agent, but also aids in ionic transfer due to the electron-withdrawing properties of four carboxyl groups. This suggests that the role of our polymer component is much more complex than simply acting as a porous solid matrix for liquid (LiX in PC-EC) [27–28], therefore, the 10% and 20% poly (MMA-BMI) provide us with excellent values of transference number. Second, the significant difference in the transference number of the 10% and 20% PEGMEMA$_{1100}$-BMI samples (0.29 vs. 0.22) are the length of EO chain decreased the electrolyte mechanical properties and support the electrolyte contact perfectly to the electrode. However, molecular weight and ionic motion must also be considered for polymer excogitation. That means we must design the polymer structure to 10 wt.% poly (PEGMEMA$_{1100}$-BMI) for low rate application, which has an attractive power to cycle performance due to their respectable ionic transfer of low glass temperature of
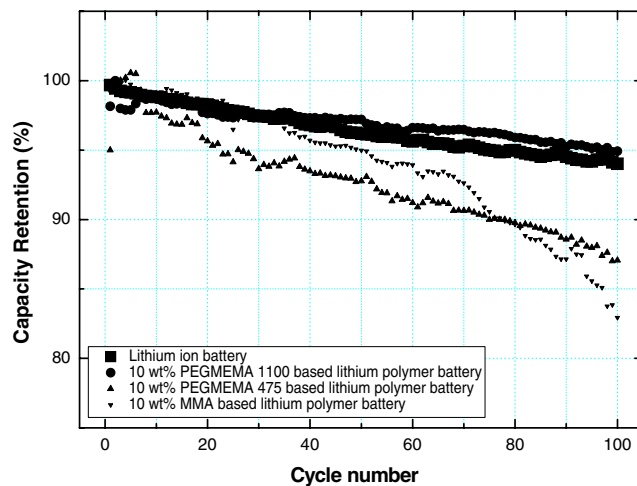
Fig. 9 The relation between load current and the capacity of the lithium ion and polymer battery with LiCoO$_2$, and MCMB. The capacity retention ratios at various discharge rates were estimated by the capacity at 0.2 °C

flexible structure instead of increasing molecular weight and decreasing ionic motion by using 20 wt.% poly (PEGMEMA$_{1100}$-BMI). Accordingly, there is the reason for the large difference in transport number for the 10% and 20% poly (PEGMEMA$_{1100}$-BMI) samples.

Cell performances of the Lithium ion polymer batteries

The c-rate performance of ALB using the gel polymer electrolytes has been investigated. Figure 8 shows the typical charge and discharge profiles of the lithium polymer battery and the average discharge voltage reached 3.7 V at 0.2 °C. The utilization of the LiCoO$_2$, MCMB with the

Fig. 8 The typical charge and discharge profile of a lithium ion battery with LiCoO$_2$, MCMB, and a 10 wt.% poly (PEGMEMA$_{1100}$-BMI) gel electrolyte. Nominal capacity 750 mAh, charge and discharge current 0.2 °C, constant current voltage 4.2 V, cut-off voltage 2.75 V

Fig. 10 Cycle performance of the lithium ion and polymer battery with LiCoO$_2$ and MCMB. Nominal capacity 750 mAh, charge and discharge current 0.2 °C, constant current voltage 4.2 V, cut-off voltage 2.75 V. The capacity retention ratio was estimated by the capacity at the second cycle

BMI-based gel electrolyte was estimated to be almost 96.8% when the initial discharge capacity was 727 mAh at 0.2 °C. The charge and discharge curves show excellent reversible capacity in the formation process. Fully charged batteries were discharged at 0.2, 0.5, 1, and 2 °C. Figure 9 shows the C-rate performance of the gel polymer electrolytes with 10 wt.% of poly (MMA-BMI), poly (PEG-MEMA$_{450}$-BMI), and poly (PEGMEMA$_{1100}$-BMI). With poly (MMA-BMI), the battery's capacity reaches 90.5% (679 mAh) at 0.2 °C. For poly (PEGMEMA$_{450}$-BMI) and poly (PEGMEMA$_{1100}$-BMI), their capacities were decreased to 655 and 727 mAh at 0.2 C, respectively. The reason for the decrease in capacity is due to the rigid structure of poly (MMA-BMI) without EO softer side chain and the also the lower ionic conductivities of poly (PEGMEMA$_{450}$-BMI) at room temperature. However, the largest EO side group will build up the three-dimensional barriers when carrier ions cannot migrate quickly in the bulk polymer electrolyte for high power application. The decreasing behavior is clearer in 2C discharge capacities decrease to 56.1% (367 mAh) for poly (PEGMEMA$_{450}$-BMI) and 65.5% (476 mAh) for poly (PEGMEMA$_{1100}$-BMI). Conclusively, the gel polymer electrolytes with high ionic conductivity and high lithium ion transport properties will be available for use in high C-rate performance.

By contrast, the poly (MMA-BMI) gel polymer battery yields a poorer cycle performance than poly (PEG-MEMA$_{450}$-BMI) and poly (PEGMEMA$_{1100}$-BMI) batteries as shown in Fig. 10. In the poly (PEGMEMA$_{1100}$-BMI) battery, the cycling stability at 100 cycles still has 94.9%. This cycle performance is most likely to the liquid-type lithium ion battery. This phenomenon is due to the longer EO chains of poly (PEGMEMA$_{1100}$-BMI) having better contact ability between the electrolyte and the electrodes with the flexible property of polymer structure. In addition, the EO side groups assist lithium ions migrate onto the flexible backbone with its electron withdrawing ability and the evidence was indicated to cycle ability at low C discharge. These appearances between polymer structure, lithium ion transport, and battery performance will support us to design a suitable product for use.

Conclusions

The cell performance of lithium polymer batteries with a poly (acrylate-*co*-imide)-based gel electrolyte is sufficient for practical use. The GPE containing LiPF$_6$ exhibited a high ionic conductivity of 4.8×10^{-3} S/cm at 25 °C. A GPE cell of LiCoO$_2$/GPE/MCMB had an excellent charge and discharge characteristics while keeping a discharge capacity of 95% after 100 cycles at room temperature. Moreover, the

results indicating a significant decrease in transport number as the length of EO increases have important implications for the use of gel polymer electrolytes in lithium ion batteries. However, the optimal addition of EO side group will enhance the cycle ability from the above results; this GPE is expected to improve the application of a room-temperature-operation-type battery.

References

1. MacCallum JR, Vincent CA (1987) Polymer electrolyte review 1. Elsevier, London
2. MacCallum JR, Vincent CA (1989) Polymer electrolyte review 2. Elsevier, London
3. Scrosati B (1989) Application of electroactive polymers. Champan & Hall, London
4. Wakihara M, Yamamoto O (1998) Li-ion batteries fundamentals and performance. Kodansha, Tokyo
5. Allcock HR, Laredo WR, Morford RV (2001) Solid State Ion 139:27
6. Niitani T, Shimada M, Kawamura K, Kanamura K (2005) J Power Sources 146:386
7. Bamford D, Dlubek G, Reiche A, Alam MA, Meyer W, Galvosas P, Rittig F (2001) J Chemical Physics 115:7260
8. Ingram MD, Imrie CT, Stoeva ZS, Pas J, Funke K, Chandler HW (2005) J Phys Chem B Lett 109:16567
9. Morford RV, Welna DT, Kellam CE III, Hofmann MA, Allcock HR (2006) Solid State Ion 177:721
10. Maitra P, Wunder SL (2004) Electrochem Solid-State Lett 7:A88
11. Ryu HS, Ahn HJ, Kim KW, Ahn JH, Lee JY (2006) J Power Sources 153:360
12. Song MK, Cho JY, Cho BW, Rhee HW (2002) J Power Sources 110:209
13. Soo PP, Huang B, Jang Y-I, Chiang Y-M, Sadoway DR, Mayes AM (1999) J Electrochem Soc 2:146
14. Morford RV, Welna DT, Kellam CE III, Hofmann MA, Allcoc HR (2006) Solid State Ion 77:721
15. Reiter J, Vondrák J, Mička Z (2005) Electrochim Acta 50:4469
16. Akashi H, Shibuya M, Orui K, Shibamoto G, Sekai K (2002) J Power Sources 112:577
17. Ryu HS, Ahn HJ, Kim KW, Ahn JH, Lee JY (2006) J Power Sources 153:360
18. Cheng CL, Wan CC, Wang YY (2004) Electrochem Commun 6:531
19. Ren T, Ren J, Tang X (2005) Polym Int 54:185
20. Noh HG (2005) US Patent 6849362B2
21. Mahesh KPO, Alagar M (2003) J Appl Polym Sci 87:1562
22. Croce F, Gerace F, Dautzemberg G, Passerini S, Appetecchi GB, Scrosati B (1994) Electrochim Acta 39:2187
23. Abraham KM, Jiang Z, Corroll B (1997) Chem Mater 9:1978
24. Cheng CL, Wan CC, Wang YY, Wu MS (2005) J Power Sources 144:238
25. Evans J, Vincent CA, Bruce PG (1987) Polymer 28:2325
26. Abraham KM, Jiang Z, Carroll B (1997) Chem Mater 9:1978
27. Appetecchi GB (1995) Electrochim Acta 40:991
28. Croce F (1993) Chem Mater 5:1268